Electronic Supplementary Information

Molecular insights into growth and time evolution of surface states of $CsPbBr_3$ nanoparticles synthesized by scalable room temperature approach

Mariangela Giancaspro,[a,b] Roberto Grisorio,[c] Gabriele Alò,[a] Nicola Margiotta,[a] Annamaria Panniello,[b] Gian paolo Suranna,[c,d] Nicoletta Depalo,[b] Marinella Striccoli,[b,e] M. Lucia Curri,[a,c,e] Elisabetta Fanizza[a,c,e,*]

[a]Chemistry Department, University of Bari, via Orabona 4 70126 Bari (IT)

[b]CNR-Institute for chemical physical process (IPCF), via Orabona 4 70126 Bari (IT)

[c]Department of Civil, Environmental, Land, Construction and Chemistry (DICATECh), Polytechnic University of Bari, Via Orabona 4, 70125 Bari (IT)

[d]CNR-Institute of Nanotechnology (Nanotec), Via Monteroni, 73100 Lecce (IT)

[e]National Interuniversity Consortium of Materials Science and Technology, INSTM, Bari Research Unit, 70126, Bari (IT)

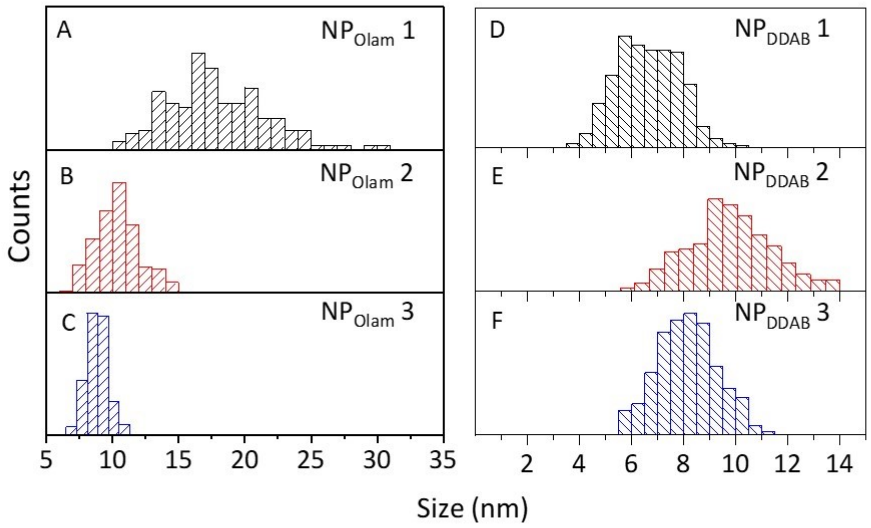

Figure S1. Statistical analysis of the size distribution of the NP_{Olam} 1-3 and NP_{DDAB} 1-3 as measured from the TEM micrographs reported in Figure 2 in the main manuscript.

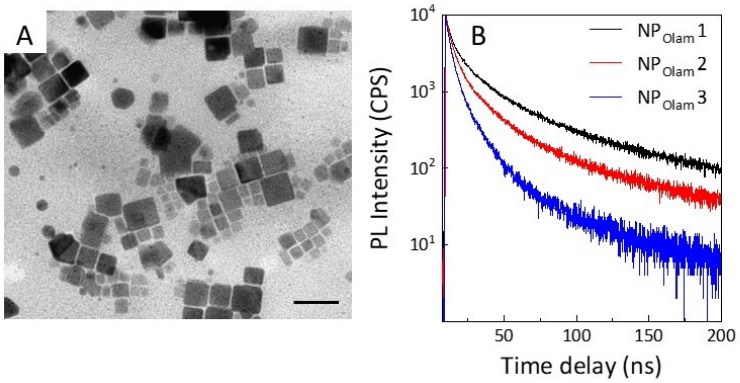

C

Sample	τ_r (ns)
NP_{Olam} 1	26.5 ± 0.4
NP_{Olam} 2	16.5 ± 0.2
NP_{Olam} 3	8.82 ± 0.2

Figure S2. (A)TEM micrograph (scale bar 50 nm) of NP_{Olam} synthesized by using nonanoic acid and purified by a two-step protocol (B) Time-resolved PL spectra of NP_{Olam} 1 (black line) NP_{Olam} 2 (red line) and NP_{Olam} 3 (blue line).

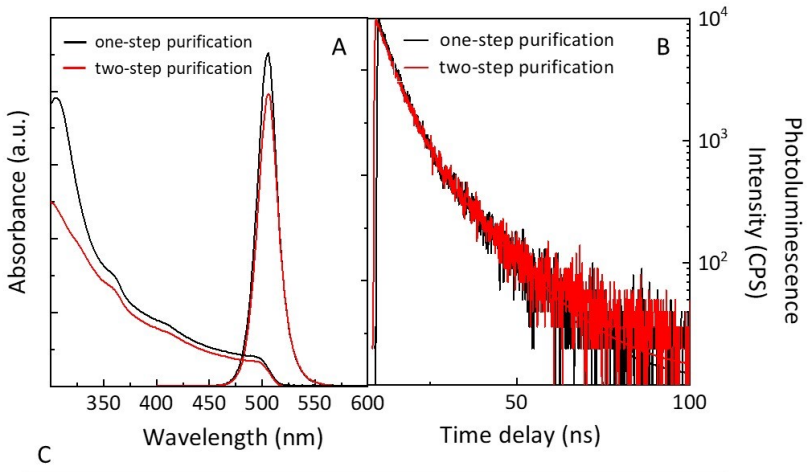

C

	NP concentration (μM)	PL QY %	<τ> ns
One-step putification	0.50	62	4.3 ± 0.2
Two-step purtification	0.45	63	5.5 ± 0.2

Figure S3. UV/Vis absorption and PL (λ_{ex} = 375nm) (A) and time-resolved PL spectra (B) of NP_{DDAB} 2 after one- (black line) and two- (red line) step purification (C) Table reporting the NP concentration and emission properties.

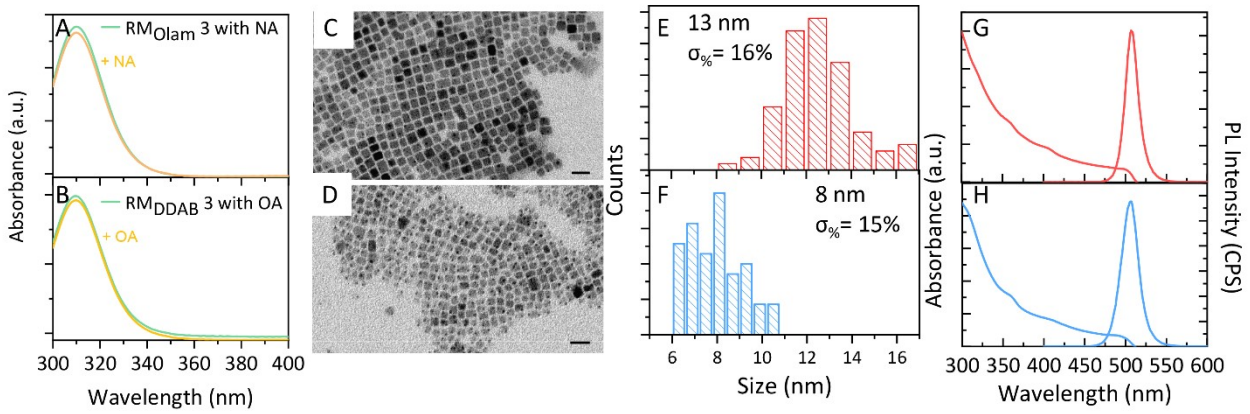

Figure S4. UV absorption spectra of the reaction mixture (RM) used for the preparation of sample NP_{Olam} 3 with NA before (green line, panel A) and after (orange line, panel A) addition of nonanoic acid (NA) solution and sample NP_{DDAB} 3 before (green line, panel B) and after (orange line, panel B) addition of oleic acid (OA) solution. TEM micrographs (C, D), statistical analysis of the size distribution (E, F) and UV-Vis absorption and emission spectra (G, H) of nanoparticles synthesized using oleyl amine (Olam) and NA (C, E, G) and didodecyl dimethyl ammonium bromide (DDAB) and OA (D, F, H).

The absorption spectrum (Figure S4 A) of the RM_{Olam} 3, prepared by replacing the oleic acid (OA) with nonanoic acid (NA), shows a lineprofile characteristic of highly coordinated bromoplumbates, even before the addition of NA solution, mimicking the cesium precursor injection. Since the NA is stronger acid than OA, it shifts the equilibria, releasing oleyl ammonium bromide and HBr. Therefore, it would be expected that NA more easily triggers the formation of highly coordinated bromoplumbates in the lead/halide reaction mixture than OA. It comes out, that the attained NPs (Figure S4 C, E) show a broad size distribution if compared to the corresponding samples achieved in the presence of OA, in agreement with the crucial role attributed to the triggering of $PbBr_6^{4-}$ bromoplumbates in the control of NP size distribution control. However, the NPs preserve the same optical properties ($\lambda_{1st\ transition}$= 501 nm, λ_{em}= 507 nm, PL QY= 45%), suggesting that the alkyl carboxylic acid, used in excess in the reaction mixtures, mainly act as activating agents in the release of the bromoplumbates, rather than taking part in direct NPs stabilization, as also confirm by NMR characterization (Figure 7, main manuscript). It has been often reported for hot injection syntheses of halide perovskite NPs [1, 2] that the length of the alkyl chain of the alkyl carboxylic acid regulates the NP size, with bigger NPs achieved using shorter alkyl chain carboxylic acid.

Conversely, the substitution of NA with OA in the synthesis carried out using didodecyl dimethyl ammonium bromide (DDAB) does not effectively change the reaction mixture composition, the size and size distribution, the optical properties of the NPs ($\lambda_{1st\ transition}$=

495 nm, λ_{em}= 505 nm, PL QY= 71%). In this case, the bromoplumbate species in this synthesis depends on the alkyl ammonium bromide content rather than being dependent on acid-base equilibrium.

Synthesis of colloidal nanoparticles in the presence of phosphorous compounds. $NP_{OPA\ DDAB}$ have been synthesized following the procedure developed by Brown et al. in toluene at room temperature.[3] Here, TOPO and OPA are used as solvation agents for $PbBr_2$ and ligands that, together with DDAB [4] are expected to passivate the $CsPbBr_3$ NPs. Different binding motif have been proposed: phosphonic moieties bound to NP surface by chelating lead ions [5, 6] or by monodentate anchoring and inter-ligand hydrogen-bonding cage of uncoordinated P-OH and P=O groups to achieve strong passivation and protection to the environment.[7] Passivation by hydrogen phosphonates, phosphonic acid anhydrides has been described to provide a strong binding to the NP surface enhancing the emission properties.[8]

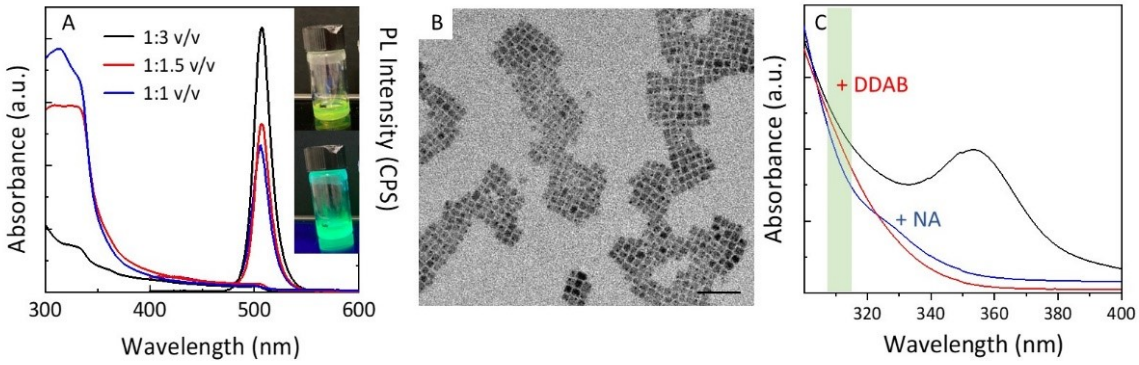

D

Sample	Size (nm)	σ (%)	ε (cm^{-1}*μM^{-1})	Concentration NP/μM	PLQY (%)	λ_{em} (nm)	FWHM (meV)
$NP_{OPA\ DDAB}$ *1*	8	13	10.2	0.042	90	503	108
$NP_{OPA\ DDAB}$ *2*	8	13	10.2	0.22	78	503	93

Figure S5. (A) UV/Vis absorption and PL spectra (λ_{ex} = 375nm) of $NP_{OPA\ DDAB}$ after one-step purification with a reaction mixture: ethyl acetate v/v ratio 1:3 (black line), 1:2 (red line) and 1:1.5 (blue line). Inset: Pictures of $NP_{OPA\ DDAB}$ after under normal indoor (top) and UV light (bottom) illumination (B) TEM micrograph (scale bar 50 nm) of $NP_{OPA\ DDAB}$ (C) UV absorption spectra of reaction mixture (RM) used for the preparation of sample $NP_{OPA\ DDAB}$ before (black line) and after (blue line) the addition of nonanoic acid (NA) solution, and after the addition of didodecyl dimethylammonium bromide (DDAB) solution (red line) (D) Table with the morphological and spectroscopic properties of the $NP_{OPA\ DDAB}$ sample prepared after two-step ($NP_{OPA\ DDAB}$ 1) and one-step ($NP_{OPA\ DDAB}$ 2) purification

Phosphine oxide coordination of cation sites and formation of hydrogen bonds between OPA and TOPO has been accounted for the good passivation and enhanced optical properties reported for this sample.[9] However, the two-step procedure used for NPs purification, bring to a poor NP production yield with NP concentration << 0.1 μM. An increase in the NP production yield above 0.2 μM became feasibly attained by reducing the extent of purification purposely balancing the amount of EtAc to reaction mixture v/v[10] to effectively remove side-products and unreacted reagents. Nanocubes with 8 nm average lateral size and σ%=13% have been synthesized following this synthetic/purification protocol, showing bright green emission centred at 503 nm (FWHM = 93 meV), with a very high PLQY of nearly 78%. The spectroscopic characterization of the RM for $NP_{OPA\ DDAB}$ at each stage of the reaction (addition of NA solution followed by addition of DDAB) reveals the presence of $PbBr_3^-$ and $PbBr_2$ bromoplumbates species absorbing at 350 nm in the as prepared RM. The absorption feature shifts to lower wavelength probably belonging to $PbBr_5^{3-}$, with a shoulder at 325 nm, corresponding to $PbBr_6^{4-}$. Therefore, the injection of cesium-nonanoate triggers the formation of $PbBr_6^{4-}$, even at a lower extent, and quite monodispersed NPs are formed. Further addition of DDAB let the absorption shoulder to completely disappears and NPs nucleation is thus expected to be quenched.

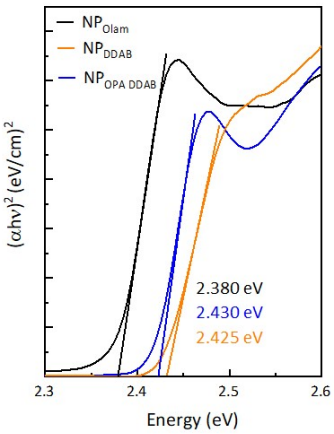

Figure S6. Tauc plots of NP_{Olam} (black line), NP_{DDAB} (orange line) and $NP_{OPA\ DDAB}$ (blue line)

	Atomic percentage		
	NP_{Olam}	NP_{DDAB}	$NP_{OPA\ DDAB}$
Pb	0.93	2.90	0.16
Cs	0.67	4.1	0.24
Br	4.49	17.1	1.11
N	9.03	9.2	16.1
P	-	-	2.02
C	78.30	62.27	76.39
	Atomic ratio Cs : Pb : Br		
$CsPbBr_3$	0.7:1:5	1.4:1:6	1.5:1:7

Figure S7. Semiquantitative analysis of the atomic percentage as measured from Energy dispersive X-ray (EDX) spectra of NP_{Olam}, NP_{DDAB}, and $NP_{OPA\ DDAB}$

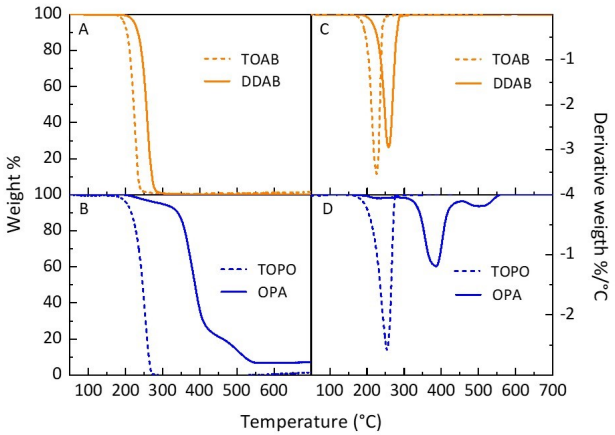

Comment [MS]: Sarebbe meglio nella figura inserire tutti a destra i valori del band gap, anche per Npolam, e soprattutto riportare sempre l'unità di misura accanto (2.380 eV)

Comment [MG]: Risolto

Figure S8. (A, B) Thermogravimetric and (C, D) first derivative curves of tetraoctylammonium bromide (TOAB), dimethyl didodecylammonium bromide (DDAB), trioctylphosphine oxide (TOPO), octylphosphonic acid (OPA) in the temperature range of 50-700°C.

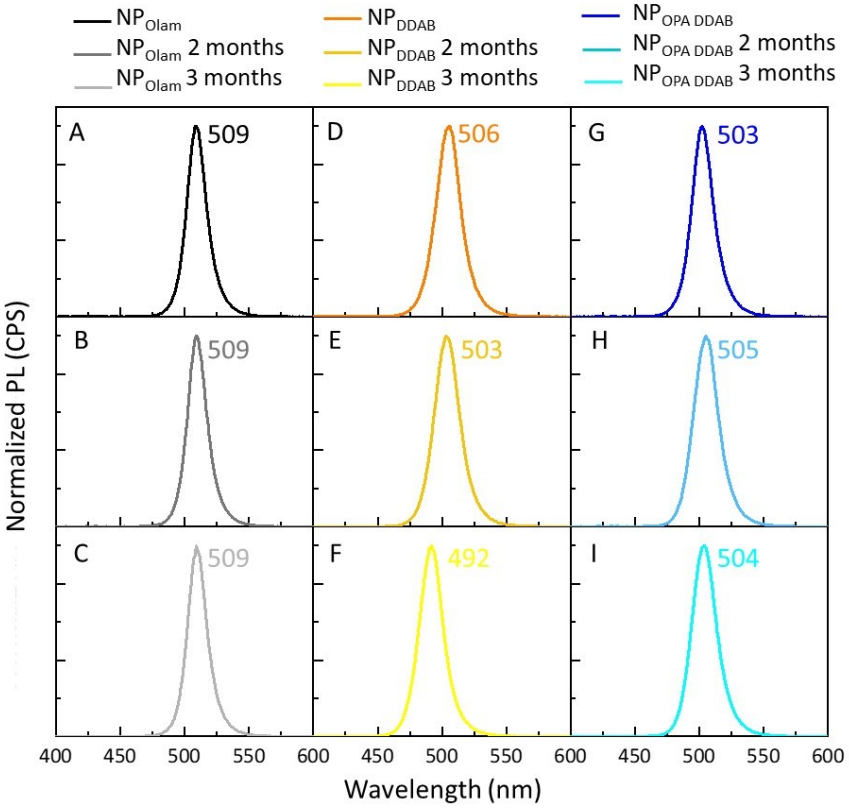

Figure S9. (A-I) Normalized PL (λ_{ex}=375nm) of (A-C) NP_{Olam}, (D-F) NP_{DDAB}, (G-I) $NP_{OPA\ DDAB}$ stored under ambient conditions for three months

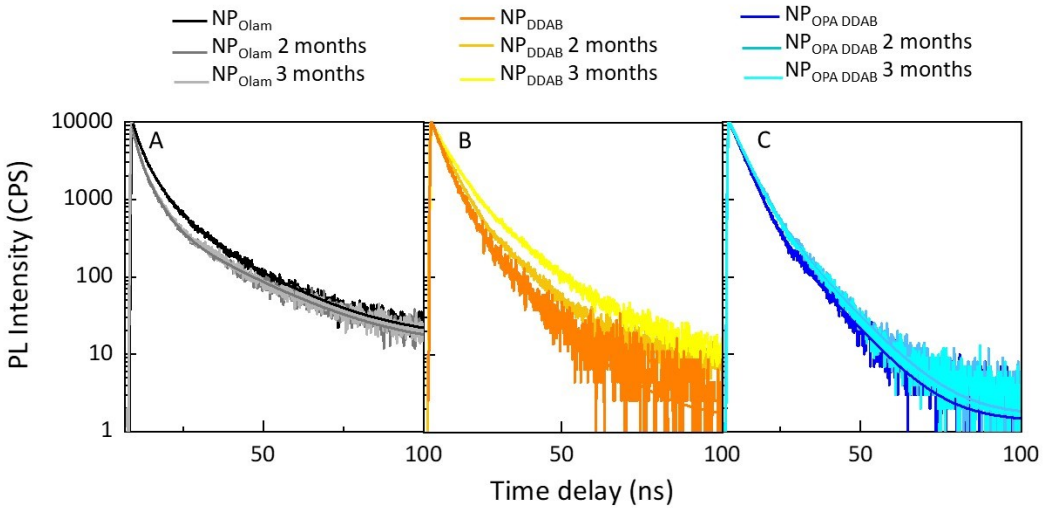

Figure S10. (A-C) Time-resolved PL spectra of (A) NP_{Olam}, (B) NP_{DDAB}, and (C) $NP_{OPA\ DDAB}$ of the different samples stored under ambient conditions over a period of three months.

	λ_{em} (nm)	FWHM (meV)	PLQY (%)	<τ> (ns)
NP_{Olam}	509	86	46±5	8.8±0.3
NP_{Olam} *2 months*	509	86	43±5	8.3±0.3
NP_{Olam} *3 months*	509	81	40±5	8.1±0.3
NP_{DDAB}	506	112	63±3	5.5±0.2
NP_{DDAB} *2 months*	503	113	79±5	6.2±0.2
NP_{DDAB} *3 months*	492	108	88±5	8.9±0.4
$NP_{OPA\ DDAB}$	503	93	78±4	5.3±0.2
$NP_{OPA\ DDAB}$ *2 months*	505	100	61±5	6.0±0.2
$NP_{OPA\ DDAB}$ *3 months*	504	100	68±5	5.8±0.2

Figure S11. Table displaying PL emission maximum, full width at half maximum (FWHM), average decay lifetime (<τ>) for NP_{Olam}, NP_{DDAB}, and $NP_{OPA\ DDAB}$ samples stored under ambient conditions for three months.

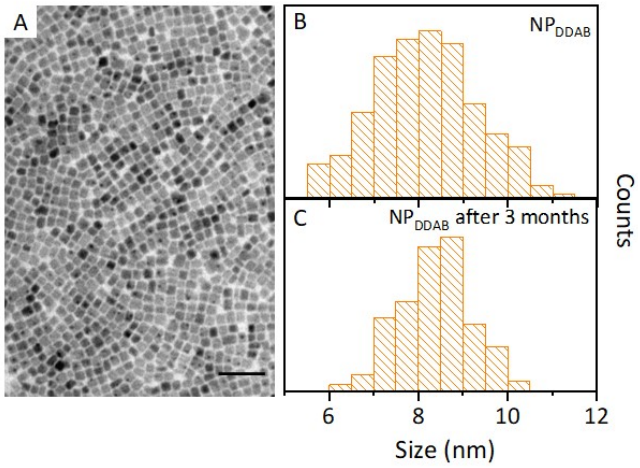

Figure S12. (A) TEM micrograph (scale bar 50 nm) of NP_{DDAB} sample after three months of storage in ambient condition and (B) statistical analysis of the size and size distribution of the as-prepared (B, Figure 2F in the main paper) and aged (C) samples.

References

1. F. Haydous, J. M. Gardner and U. B. Cappel, The impact of ligands on the synthesis and application of metal halide perovskite nanocrystals, *Journal of Materials Chemistry A*, 2021, **9**, 23419-23443.
2. M. Kazes, T. Udayabhaskararao, S. Dey and D. Oron, Effect of Surface Ligands in Perovskite Nanocrystals: Extending in and Reaching out, *Accounts of Chemical Research*, 2021, **54**, 1409-1418.
3. A. A. M. Brown, P. Vashishtha, T. J. N. Hooper, Y. F. Ng, G. V. Nutan, Y. Fang, D. Giovanni, J. N. Tey, L. Jiang, B. Damodaran, T. C. Sum, S. H. Pu, S. G. Mhaisalkar and N. Mathews, Precise Control of CsPbBr3 Perovskite Nanocrystal Growth at Room Temperature: Size Tunability and Synthetic Insights, *Chemistry of Materials*, 2021, **33**, 2387-2397.
4. Y. Shynkarenko, M. I. Bodnarchuk, C. Bernasconi, Y. Berezovska, V. Verteletskyi, S. T. Ochsenbein and M. V. Kovalenko, Direct Synthesis of Quaternary Alkylammonium-Capped Perovskite Nanocrystals for Efficient Blue and Green Light-Emitting Diodes, *ACS Energy Letters*, 2019, **4**, 2703-2711.
5. Y. Tan, Y. Zou, L. Wu, Q. Huang, D. Yang, M. Chen, M. Ban, C. Wu, T. Wu, S. Bai, T. Song, Q. Zhang and B. Sun, Highly Luminescent and Stable Perovskite Nanocrystals with Octylphosphonic Acid as a Ligand for Efficient Light-Emitting Diodes, *ACS Applied Materials & Interfaces*, 2018, **10**, 3784-3792.

6. F. Zaccaria, B. Zhang, L. Goldoni, M. Imran, J. Zito, B. van Beek, S. Lauciello, L. De Trizio, L. Manna and I. Infante, The Reactivity of CsPbBr3 Nanocrystals toward Acid/Base Ligands, *ACS Nano*, 2022, **16**, 1444-1455.
7. A. A. M. Brown, T. J. N. Hooper, S. A. Veldhuis, X. Y. Chin, A. Bruno, P. Vashishtha, J. N. Tey, L. Jiang, B. Damodaran, S. H. Pu, S. G. Mhaisalkar and N. Mathews, Self-assembly of a robust hydrogen-bonded octylphosphonate network on cesium lead bromide perovskite nanocrystals for light-emitting diodes, *Nanoscale*, 2019, **11**, 12370-12380.
8. B. Zhang, L. Goldoni, C. Lambruschini, L. Moni, M. Imran, A. Pianetti, V. Pinchetti, S. Brovelli, L. De Trizio and L. Manna, Stable and Size Tunable CsPbBr3 Nanocrystals Synthesized with Oleylphosphonic Acid, *Nano Letters*, 2020, **20**, 8847-8853.
9. B. Zhang, L. Goldoni, J. Zito, Z. Dang, G. Almeida, F. Zaccaria, J. de Wit, I. Infante, L. De Trizio and L. Manna, Alkyl Phosphonic Acids Deliver CsPbBr3 Nanocrystals with High Photoluminescence Quantum Yield and Truncated Octahedron Shape, *Chemistry of Materials*, 2019, **31**, 9140-9147.
10. R. Grisorio, D. Conelli, R. Giannelli, E. Fanizza, M. Striccoli, D. Altamura, C. Giannini, I. Allegretta, R. Terzano and G. P. Suranna, A new route for the shape differentiation of cesium lead bromide perovskite nanocrystals with near-unity photoluminescence quantum yield, *Nanoscale*, 2020, **12**, 17053-17063.